

UDC 539.3

## MODELLING OF PSEUDOELASTIC SMA BEHAVIOUR UNDER COMBINED LOADING

Vasyl Voronchak; Volodymyr Iasnii

*Ternopil Ivan Puluj National Technical University, Ternopil, Ukraine*

**Abstract.** The behaviour of pseudoelastic nickel-titanium alloy  $Ni_{55.75}Ti_{44.15}$  under tension, bending, and their simultaneous action is investigated in this paper. The methodology for modelling the mechanical properties of SMAs under various loading conditions, including combined loading, is proposed. The stresses of forward and reverse phase transformations between austenite and martensite are determined using ANSYS software based on the finite element method. The obtained modelling results confirm high adaptability of SMA to various types of loadings. These investigations are required for more efficient design of structures and devices and for predicting the behaviour of pseudoelastic SMAs under different types of loading.

**Key words:** pseudoelasticity, shape memory alloys, modelling, phase transformational stresses, combined loading.

[https://doi.org/10.33108/visnyk\\_tntu2025.01.132](https://doi.org/10.33108/visnyk_tntu2025.01.132)

Received 28.11.2024

### 1. INTRODUCTION

Shape memory alloys (SMAs) are a unique class of materials that have the property to restore their original shape after deformation under thermomechanical loading or heating [1–2]. Due to their ability to transform, these materials play a key role in many high-tech industries, including aerospace, medical, automotive, robotics, etc. [3–6]. The SMA peculiarity is characterised by forward and reverse phase transformations between martensite and austenite, which depend on temperature – the shape memory effect (Fig. 1 a) and stresses – pseudoelasticity (Fig. 1 b). The main mechanisms that change the behaviour of alloys under combined loading, particularly tensile bending, include the simultaneous influence on phase transformations and mechanical reorganisation of the martensite structure. Tensile bending is the common complex loading for many real structures in medicine, bioengineering, mechanical engineering, and construction.

The phase transformations of SMAs are based on the unique property of the material to change the crystal structure under the influence of temperature or mechanical loading [7–10]. The main phases in SMA are austenite (high-temperature phase) and martensite (low-temperature phase). These phases have different crystal structures: austenite is usually characterized by cubic structure, while martensite is tetragonal.

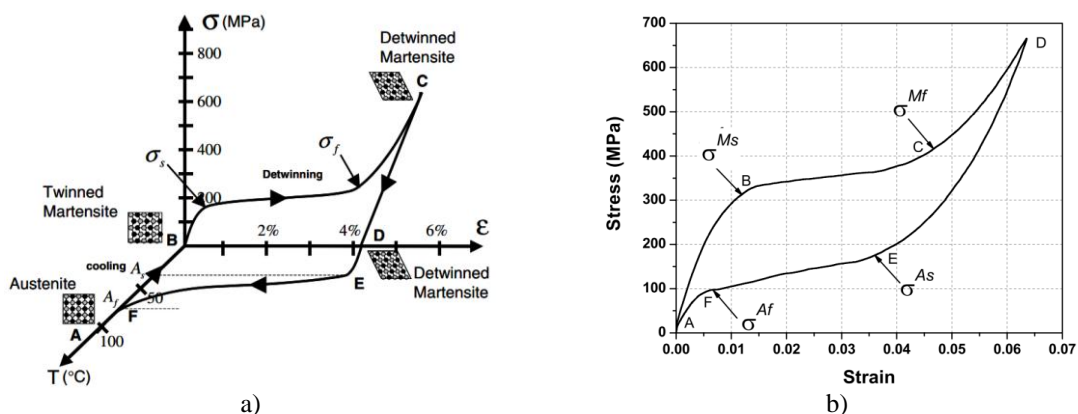


**Figure 1.** The influence of stress, strain and temperature reflecting the shape memory effect (a) and pseudo-elastic state (b) for NiTi alloys [11]

Due to their phase transformation, shape memory alloys provide unique opportunities for creating active damping systems that respond to environmental changes or external influences [11].

The total strain of  $\varepsilon$  nickel-titanium alloy is determined by the following formula:

$$\varepsilon = \varepsilon_e + \varepsilon_t + \varepsilon_p \quad (1)$$

where  $\varepsilon_e$  is the elastic strain;  $\varepsilon_t$  is the transformational deformation;  $\varepsilon_p$  is the plastic deformation.

The transformational deformation is considered as:

$$\varepsilon_t = \varepsilon_L x^S N_t \quad (2)$$

where:  $\varepsilon_L$  is the material parameter characterising maximum transformational deformation;  $x^S$  is the volume fraction of martensite;  $N_t$  is the direction of transformational deformation.

The stressed state of the SMA is caused by the change in phase composition. The stress equations take into account the interaction of elasticity, plasticity and phase transformation typical for shape memory alloys. They are generally defined as follows:

$$\sigma = f(E, T, \xi, A) \quad (3)$$

where  $\sigma$  is the stress,  $f$  is the function that takes into account elasticity, plasticity and phase transformations,  $E$  is the elasticity modulus,  $T$  is the temperature,  $\xi$  is the volume fraction of martensite,  $A$  is the direction of transformational deformation.

Additionally, the stresses at phase transformations can be described by the following formulas:

The beginning of the martensitic transformation is expressed by the formula:

$$\sigma^{Ms} = C_M (T - M_s) \quad (4)$$

where:  $C_M$  is the coefficient of stress influence on martensitic transformation,  $T$  is the temperature,  $M_s$  is the temperature of the martensitic transformation beginning.

The completion of the martensitic transformation can be described by the following formula:

$$\sigma^{Mf} = \sigma^{Ms} - \Delta\sigma \quad (6)$$

The beginning of the austenitic transformation is expressed by the formula:

$$\sigma^{As} = C_A (T - A_s) \quad (7)$$

The completion of the austenitic transformation is calculated according to the formula:

$$\sigma^{Af} = \sigma^{As} + \Delta\sigma \quad (8)$$

where  $\Delta\sigma$  is the difference between the stress at the end and beginning of the phase transformation. These formulas describe the main characteristics of stresses in shape memory

alloys during phase transformations and are the main ones for calculating their mechanical behaviour [12, 13].

This paper is devoted to the modelling and analysis of the SMA behaviour under tensile, bending and their combined action. The investigation is required to extend the scope of SMAs application and to predict the behaviour of such materials under the influence of operational loading modes in real structures. This makes it possible to create more efficient structures and systems based on SMA.

## 2. EXPERIMENTAL METHODS

The SMA behaviour was modelled using ANSYS 2024 R2 finite element analysis (FEA) software. The sample model was created and the corresponding properties of nickel-titanium alloy (Ni<sub>55,75</sub>Ti<sub>44,15</sub>) were set (Fig. 2).

	A	B	C	D	E
1	Property	Value	Unit		
2	Material Field Variables	Table			
3	Density	6,45	g cm <sup>-3</sup>		
4	Isotropic Elasticity				
5	Derive from	Youn...			
6	Young's Modulus	72400	MPa		
7	Poisson's Ratio	0,36			
8	Bulk Modulus	8,619E+10	Pa		
9	Shear Modulus	2,6618E+10	Pa		
10	Superelasticity				
11	Sigma SAS	332	MPa		
12	Sigma FAS	368	MPa		
13	Sigma SSA	174	MPa		
14	Sigma FSA	103	MPa		
15	Epsilon	0,054	m m <sup>-1</sup>		
16	Alpha	0			
17	Es	18700	MPa		

**Figure 2.** Properties of Ni<sub>55,75</sub>Ti<sub>44,15</sub> in ANSYS environment

Mechanical properties of the SMA were taken from the experimental study [14], which were determined under uniaxial tension according to the standard [15]. According to this standard, the material is first stretched to 6% strain, then unloaded to the stress less than 7 MPa, and then stretched until the sample failure, as described in the paper [14].

The diameter of the sample used to model the SMA behaviour is 4 mm, and the length of the operating area is 12.5 mm. The total length of the sample is 46 mm (Fig. 3a). The calculation scheme of the modelled sample is as follows: the sample is rigidly fixed on one side, and the displacement is set on its opposite side. The finite element model of the sample in the ANSYS environment, where the plane of the sample fixation, position A (blue), is shown in Fig. 3b. On the opposite side, position B (yellow), the plane with the shifted movement is depicted.

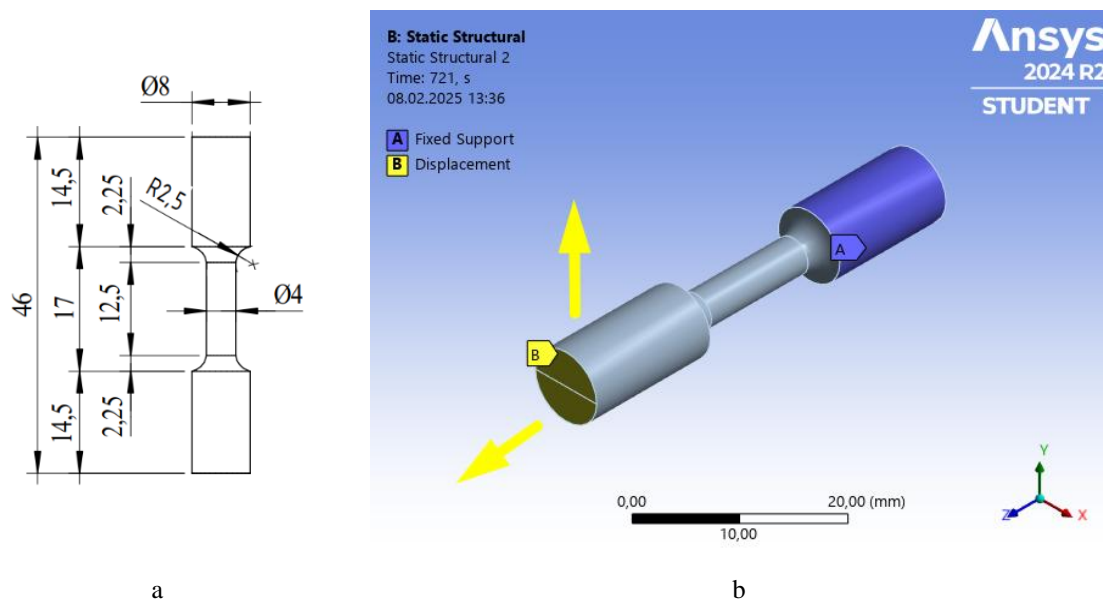


**Figure 3.** Test sample: a) sketch of geometric dimensions;  
b) finite element model in ANSYS environment

Similarly to the experimental investigations, the ambient temperature was 18.8°C [14].

The behaviour of nickel-titanium alloy was determined under three loading conditions (Fig. 4): uniaxial tension, bending and their simultaneous action (tension with bending). In all cases, the maximum strain was 6%.

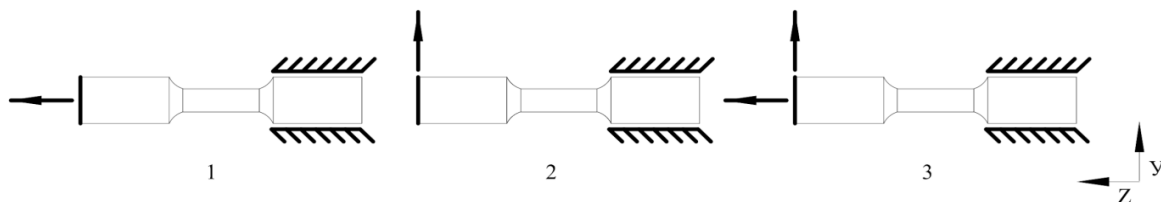


**Figure 4.** Calculation schemes of the model: 1) in case of tension; 2) in case of bending;  
3) in case of combined action of tension and bending.

The applied displacement in the Z-axis direction, according to the tensile modelling of the sample, was 0.64 mm, corresponding to 4.52 kN force, and in the Y-axis direction for bending, the displacement was 4.5 mm, corresponding to 0.14 N force. For combined loading, the displacement in the Z-axis direction was 0.14 mm, corresponding to 2.36 kN force, and the displacement in the Y-axis direction was 0.97 mm, corresponding to 0.55 kN force.

### 3. RESULTS AND DISCUSSIONS

Taking into account SMA peculiarities, one of the most important parameters characterizing their properties and determining the area of application are the stresses of forward and reverse phase transformations.

The results of the stress-strain modelling and the results of experimental investigations of tensile SMA samples are shown in Fig. 5. The results of experimental investigations of SMA samples are taken from the paper [14].

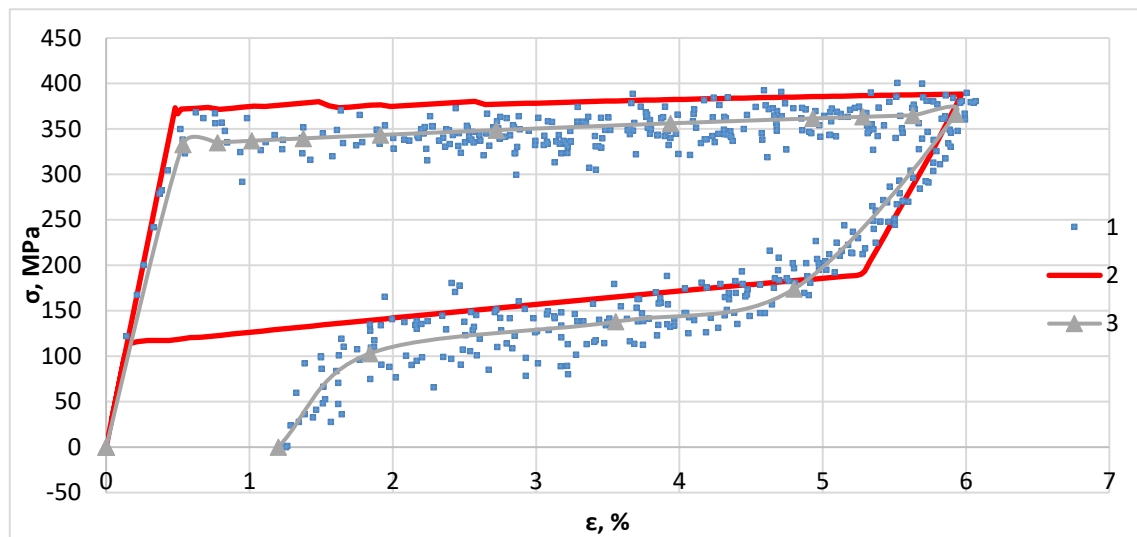


**Figure 5.** Diagram of the dependence of normal stresses on strain: 1) during experimental investigation [14]; 2) while modelling; 3) approximation of experimental investigations

The modelling results show (Fig. 5) that the stresses of direct phase transformation from austenite to martensite are  $\sigma^{Ms}=366$  MPa and  $\sigma^{Mf}=388$  MPa, and the stresses of unloaded (reverse) phase transformation are  $\sigma^{As}=190$  MPa and  $\sigma^{Af}=113$  MPa. During the experimental investigations, the stresses of forward phase transformation from austenite to martensite were  $\sigma^{Ms}=332$  MPa and  $\sigma^{Mf}=368$  MPa, and under unloaded (reverse) conditions  $\sigma^{As}=174$  MPa and  $\sigma^{Af}=103$  MPa.

To sum up, we can note that the stress at the beginning of forward phase transformation  $\sigma^{Ms}$  during modelling is 10.24% higher than in the experimental investigation, and the stress at the end of forward phase transformation  $\sigma^{Mf}$  is 9.19% higher than in the experimental investigation. For the reverse phase transformation, the beginning stress  $\sigma^{As}$  is 1.15% higher than in the experimental investigation, and the final stress  $\sigma^{Af}$  is 9.70% higher as well. Small discrepancy between the values indicates satisfactory data convergence.

The modelling results of the stress-strain state under tension, bending and combined loading (simultaneous action of tension and bending) are shown in Figure 6.

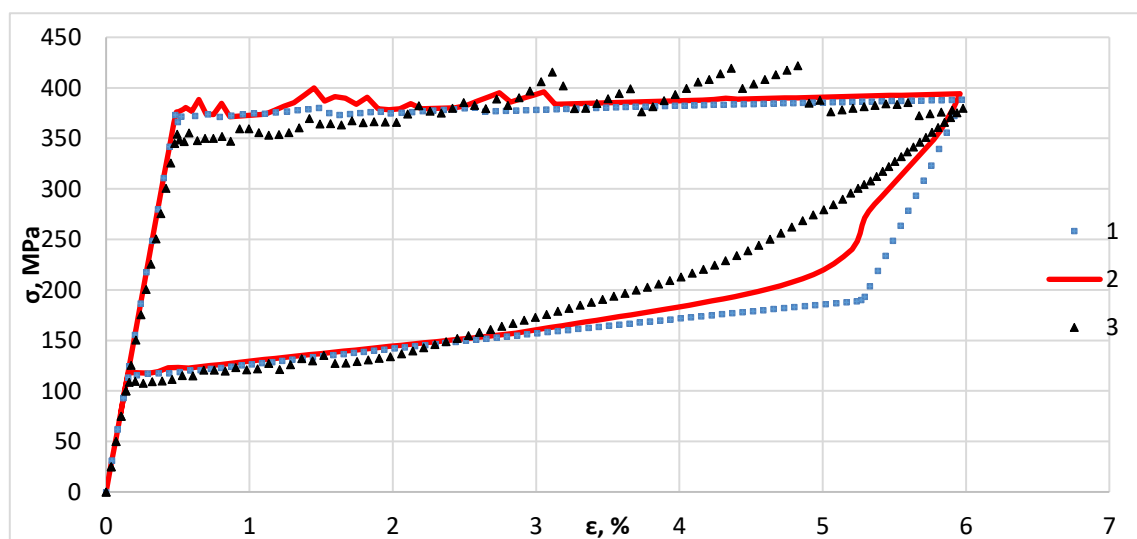


**Figure 6.** Diagram of the dependence of normal stresses on deformation: 1) in case of tension; 2) in case of bending; 3) in case of combination

The results are presented as the dependence of normal stresses in the Z-axis direction on total deformations (Equivalent Total Strain). It should be noted that with forward phase transformations, the stress values  $\sigma^{Ms}$  and  $\sigma^{Mf}$  for all types of loads are practically the same. During reverse transformation under tension, the stress-strain dependences manifest linear behaviour compared to bending and their combinations. This deviation can be explained by the higher value of the applied displacement, which can cause the simultaneous occurrence of tension and compression areas.

The generalized results of the SMA modelling SDS are given in Table 1.

**Table 1**

Obtained results of SDS SMA

Type of loading	$\Delta_z$	$\Delta_y$	$\varepsilon$ , %	$\sigma^{Ms}$	$\sigma^{Mf}$	$\sigma^{As}$	$\sigma^{Af}$	Total force, kN
	mm			MPa				
Tension	0.64	–	5.97	366	388	190	113	4.52
Bending	–	4.5	5.96	365	394	220	117	0.14
Tension with bending	0.14	0.9675	5.98	354	379	200...220	108	2.9

The obtained results of FEM modelling make it possible to determine the phase transformation stresses and to set the displacement for the SMA sample corresponding to 6% strain. Under the given loading parameters, forward and reverse phase transformations occur, with the strain of 6% not exceeding the value at which the functional properties of the SMA deteriorate significantly.

#### 4. CONCLUSION

The SMA behaviour is modelled under tensile and bending actions and under their combined action. Forward and reverse transformation stresses are determined. The modelling results confirm the high adaptability of the SMA to various types of loadings. Understanding of these peculiarities makes it possible to design structures more efficiently and predict the behaviour of nickel-titanium alloys under various mechanical impacts, making them promising for use in seismic structures, adaptive mechanisms, and other high-tech industries.

#### References

1. Kumar P. K., Lagoudas D. C. "Shape Memory Alloys", 2008, pp. 433.
2. Fang C. et al. (2019) Superelastic NiTi SMA cables: Thermal-mechanical behavior, hysteretic modelling and seismic application. *Eng. Struct.*, vol. 183, pp. 533–549. <https://doi.org/10.1016/j.engstruct.2019.01.049>
3. Hartl D., Volk B., Lagoudas D. C., Calkins F. T., Mabe J., Thermomechanical characterization and modeling of Ni60Ti40 SMA for actuated chevrons, in: *Proceedings of ASME, International Mechanical Engineering Congress and Exposition (IMECE)*, 5–10 November, Chicago, IL, 2006, pp. 1–10. <https://doi.org/10.1115/IMECE2006-15029>
4. Fang C. (2022) SMAs for infrastructures in seismic zones: A critical review of latest trends and future needs. *Journal of Building Engineering*, vol. 57, p. 104918. <https://doi.org/10.1016/j.job.2022.104918>
5. Ajaj R. M., Parancheerivilakkathil M. S., Amoozgar M., Friswell M. I., Cantwell W. J. (2021) Recent developments in the aeroelasticity of morphing aircraft. *Progress in Aerospace Sciences*, vol. 120, p. 100682. <https://doi.org/10.1016/j.paerosci.2020.100682>
6. Iasnii V., Yasniy O., Homon S., Budz V., Yasniy P. (2023) Capabilities of self-centering damping device based on pseudoelastic NiTi wires. *Engineering Structures*, vol. 278, p. 115556. <https://doi.org/10.1016/j.engstruct.2022.115556>

7. Mabe J., Ruggeri R., Calkins F. T., (2006) Characterization of nickel-rich nitinol alloys for actuator development, in: Proceedings of the International Conference on Shape Memory and Superelasticity Technology.
8. Clingman D. J., Calkins F. T., Smith J. P., (2003) Thermomechanical properties of 60-Nitinol, in: Proceedings of the SPIE, Smart Structures and Materials: Active Materials: Behavior and Mechanics, vol. 5053, pp. 219–229. <https://doi.org/10.1117/12.498548>
9. Longhuan Tian, Jianyou Zhou, Pan Jia, Zheng Zhong (2024) Thermomechanical response and elastocaloric effect of shape memory alloy wires. Mechanics of Materials, vol. 193, p. 104985. <https://doi.org/10.1016/j.mechmat.2024.104985>
10. Iasnii V. P., Junga R. (2018) Phase Transformations and Mechanical Properties of the Nitinol Alloy with Shape Memory. Materials Science, vol. 54, no. 3, pp. 406–411. <https://doi.org/10.1007/s11003-018-0199-7>
11. Miller D. A., Lagoudas D. C. (2000) Thermomechanical characterization of NiTiCu and NiTi SMA actuators: influence of plastic strains. Smart Mater. Struct., vol. 9, no. 5, p. 640. <https://doi.org/10.1088/0964-1726/9/5/308>
12. Yang J. H., Wayman C. M. (1992) Self-accommodation and shape memory mechanism of  $\epsilon$ -martensite-I. Experimental observations. Mater. Charact. Elsevier, vol. 28, no. 1, pp. 23–35. [https://doi.org/10.1016/1044-5803\(92\)90026-E](https://doi.org/10.1016/1044-5803(92)90026-E)
13. Otsuka K., Wayman C. M. Shape Memory Materials. Cambridge University Press, Cambridge, UK, pp. 1998–267.
14. Bykiv N., Iasnii V., Yasniy P., Junga R. (2021) Thermomechanical analysis of nitinol memory alloy behavior. Scientific journal of TNTU, vol. 102, pp. 161–167. [https://doi.org/10.33108/visnyk\\_tntu2021.02.161](https://doi.org/10.33108/visnyk_tntu2021.02.161)
15. ASTM F2516-22. Standard Test Method for Tension Testing of Nickel-Titanium Superelastic Materials. Book of Standards Volume: 13.02.2022.

## УДК 539.3

## МОДЕЛЮВАННЯ ПОВЕДІНКИ ПСЕВДОПРУЖНОГО СПФ ЗА СКЛАДНОГО НАВАНТАЖЕННЯ

Василь Ворончак; Володимир Ясній

Тернопільський національний технічний університет імені Івана Пулюя,  
Тернопіль, Україна

**Резюме.** Досліджено поведінку псевдопружного нікель-титанового сплаву з пам'яттю форми  $Ni_{55,75}Ti_{44,15}$  методом скінченних елементів за різних типів навантаження. У середовищі ANSYS запропоновано методику моделювання механічних властивостей СПФ та визначення напружень прямих і зворотних фазових перетворень. Діаметр зразка для моделювання поведінки складає 8 мм з робочою ділянкою діаметром 4 мм та довжиною 12,5 мм. Прикладене переміщення за одновісного розтягу, згину та їх одночасної дії (розтяг зі згином), спричиняло деформацію, що не перевищувала значення 6%. Результати досліджень показали, що при розтягу значення прямих фазових перетворень СПФ з аустеніту в мартенсит становлять  $\sigma^{Ms} = 366$  МПа та  $\sigma^{Mf} = 388$  МПа. При розвантаженні значення зворотних перетворень дорівнюють 190 МПа та 113 МПа відповідно. Дослідження також показало, що для згину та комбінованого навантаження значення фазових перетворень з аустеніту в мартенсит  $\sigma^{Ms}$  та  $\sigma^{Mf}$  практично однакові. При зворотному перетворенні за розтягу, залежності напруження від деформацій демонструють лінійну поведінку в порівнянні зі згином чи комбінованому навантаженні, що пояснюється перерозподілом напружень між різними зонами деформації та різним значенням прикладеного переміщення. Порівняльний аналіз результатів моделювання та експериментальних даних показав, що розбіжність становить до 10%. Це свідчить про достатню збіжність отриманих значень. Отримані результати моделювання підтверджують високу адаптивність псевдопружних СПФ до різних типів навантажень та можливість їх застосування в різноманітних пристроях чи конструкціях, що експлуатуються за дії складного навантаження. Ці дослідження є необхідними для ефективного проектування конструкції та пристроїв, а також для прогнозування поведінки псевдопружних сплавів з пам'яттю форми під дією різних типів навантаження.

**Ключові слова:** псевдопружність, сплави з пам'яттю форми, моделювання, напруження фазових перетворень, складне навантаження.

[https://doi.org/10.33108/visnyk\\_tntu2025.01.132](https://doi.org/10.33108/visnyk_tntu2025.01.132)

Отримано 28.11.2024